

# Prediction of Remaining Life of Turbo Pump Inducer for Spacecraft Using Cumulative Damage Model

Hatsuo Mori<sup>1</sup>, Makoto Imamura<sup>2</sup>

<sup>1</sup>*IHI corporation, Tokyo, 190-1297, Japan  
Mori7953@ihi-g.com*

<sup>2</sup>*Tokai University, Tokyo, 108-0074, Japan  
imamura@tsc.u-tokai.ac.jp*

## ABSTRACT

In the near future, to operate reusable spacecraft safely and efficiently, it is necessary to have failure prediction technology for reusable rocket engines. Among the components that constitute a rocket engine, the failure of the turbo pump inducer has a significant impact on missions. Therefore, we have been researching to monitor the remaining life of the inducer.

This method estimates the fluctuating stress field excited in the inducer section based on the time-series signals from pressure sensors installed upstream. It predicts the remaining life using a Rain flow model to account for high-cycle fatigue (HCF) phenomena. To validate the effectiveness of the proposed method, we attempted to acquire experimental data, particularly for the challenging pressure-stress transfer section where concrete specifications are difficult to define. Through experiments using an elemental model, we demonstrated that a certain degree of remaining life can be predicted based on measurement from the upstream sensor.

This indicates that the proposed method is a promising option for solving the remaining life prediction problem of reusable spacecraft.

## 1. INTRODUCTION

The development of reusable space transport vehicles is being pursued to achieve low-cost and high-frequency space utilization. Health monitoring is required for such reusable launch vehicles to safely return to the ground even if the launch mission cannot be accomplished owing to any unexpected event during the flight. The rocket engine, a major component of the rocket, is a complex system, and automating its health monitoring is an important challenge.

---

First Author et al. This is an open-access article distributed under the terms of the Creative Commons Attribution 3.0 United States License, which permits unrestricted use, distribution, and reproduction in any medium, provided the original author and source are credited.

The role of health monitoring can be divided into 2 categories; (1) detecting the signs of failure and (2) monitoring the accumulation of fatigue and (2) is focused in this paper. Previous studies have been conducted on the combustion chamber, which is exposed to high temperatures, focusing on thermal stress and creep, by Sato (2019) and Chelouati, M., Jha, M. S., Galeotta, M., & Theilliol, D. (2021). The turbo pump is also the component operated in extreme environments, where high temperatures, high pressures, extreme cold, and high rotational speeds coexist. Consequently, fatigue accumulates in various parts with each operation, and failure occurs when it exceeds a certain limit. While this was not a major concern in expendable rockets, knowing the remaining life becomes crucial for reusable spacecraft to avoid in-flight failures.

Among turbo pump parts used in extreme conditions, the inducer is particularly difficult to acquire data in situ. The function of the inducer is to suck the propellant and boost it up to the desired pressure required by the impeller, the main boost device installed in the line, e.g., shown in Figure 1 by Mizuno, Kobayashi, and Oguchi (2009). To reduce the weight of the propellant tanks, the inducer inlet pressure is set to be low. As a result, there is constant cavitation due to negative pressure around the inducer, and the occurrence and disappearance of cavitation generate vibration forces that lead to the destruction of the inducer blades through HCF. When the inducer fails for any reason, it can cause secondary disasters by colliding with the pipe walls or downstream components due to centrifugal forces or rotational contact. Since these events occur instantaneously, it is necessary to have a system that can monitor HCF and stop the operation preventively before the destruction occurs, rather than detecting the inducer failure and stopping the operation afterward.

In this paper, we present a partial overview of previous research on the real-time prediction of the remaining life of the inducer before reaching the point of failure. In our proposed method, the estimated fluctuating stress field

excited in the inducer is used for predicting the remaining life as an HCF phenomenon. To estimate the fluctuating stress in real-time, we use the time-series signal from pressure sensors installed upstream of the inducer.

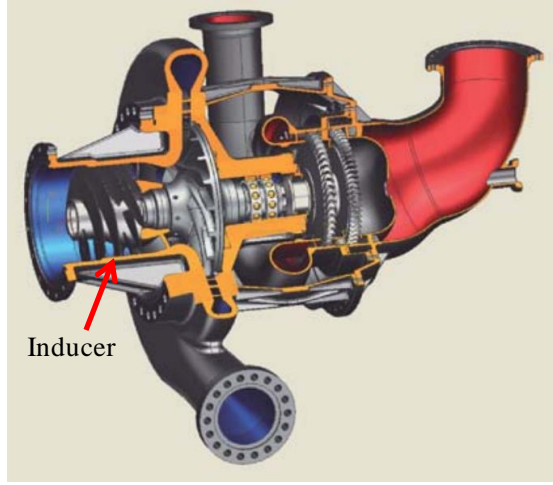


Figure 1. An example of an inducer as a spiral part of a turbo pump

## 2. NECESSITY OF REMAINING LIFE PREDICTION

It is difficult to predict instantaneous failure caused by HCF in the inducer, and there are currently no established techniques, at least in the field of rocket turbo pumps. Moreover, directly measuring the stress on the inducer, which is a thin plate component operated within cavitation, is considerably difficult in terms of sensor placement and ensuring reliability. Therefore, we try to indirectly estimate the stress based on time-series data from pressure sensors installed upstream.

## 3. PROPOSED LIFE PREDICTION METHOD

### 3.1. Remaining Life Evaluation Policy

To define the concept of remaining life prediction, we introduce the following three terms with mathematical representation.

- Cumulative fatigue damage  $\psi$ : It is the accumulation of damage from the past to the present, starts from 0, and it is considered to reach the life limit when it exceeds 1.
- Available operating time  $\frac{1-\psi}{\dot{\psi}(t)}$ : By dividing it by the consumption rate of the life  $\dot{\psi}$ , the remaining available operating time can be calculated.
- Anomaly criteria: It is determined as an anomaly if the remaining mission cannot be completed during this flight.

$$\frac{1-\psi}{\dot{\psi}(t)} + t_n = \frac{1 - (\psi_{n-1} + \Delta\psi_n(t_n))}{\dot{\psi}(t_n)} + t_n < Treq_n \quad (1)$$

$t_n$  : Cumulative local time for the n-th flight [s]

$Treq_n$  : Required service lifetime for the n-th flight [s]

$\psi_{n-1}$  : Cumulative fatigue damage up to the (n-1)-th flight [-]

$\Delta\psi_n(t)$  : Cumulative fatigue damage up to t seconds for the n-th flight [-]

$\dot{\psi}(t)$  : Current rate of life consumption [1/s]

These are illustrated in Figure 2.

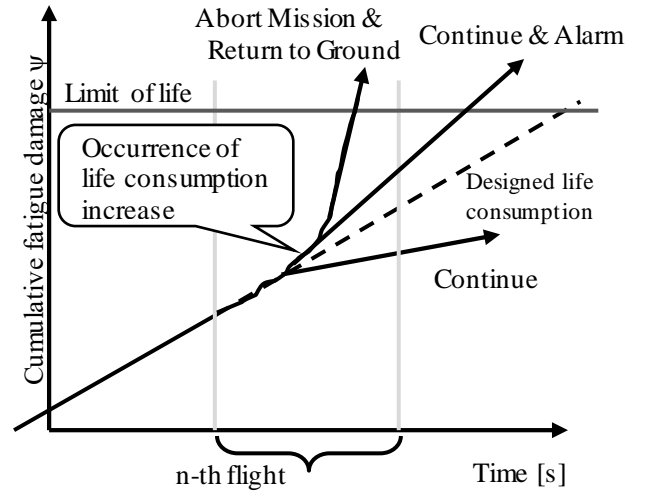


Figure 2. Image of abnormality judgment

If we define the following as the discriminant,  $D$ , then if  $D$  becomes negative, it can be judged that the life has ended. The first term on the right side represents the remaining time calculated from the current rate of life degradation, and the second term represents the elapsed time in the current flight.

$$D = \frac{1 - (\psi_{n-1} + \Delta\psi_n(t_n))}{\dot{\psi}(t_n)} + t_n - Treq_n \quad (2)$$

From the above, it is important to construct a model for calculating the cumulative fatigue damage  $\psi$  based on the measurement data during flight.

### 3.2. Input/output Identification

To develop a time-series model that outputs the cumulative fatigue damage  $\psi$ , it is necessary to clarify the various input-output relationships and identify the fixed and varying components. To clarify the scope of this paper, the following systemchart is provided.

For each set of specified inputs and fixed values shown in Figure 3, various force fields are generated around the inducer. The inducer blades respond to these fields. It is necessary to estimate or measure the transfer function that represents this response by using some method. Once the

response of the inducer is obtained as stresses (or strains), the accumulated fatigue damage can be estimated and, based on the operating conditions shown in Figure 2, predictive judgments can be made.

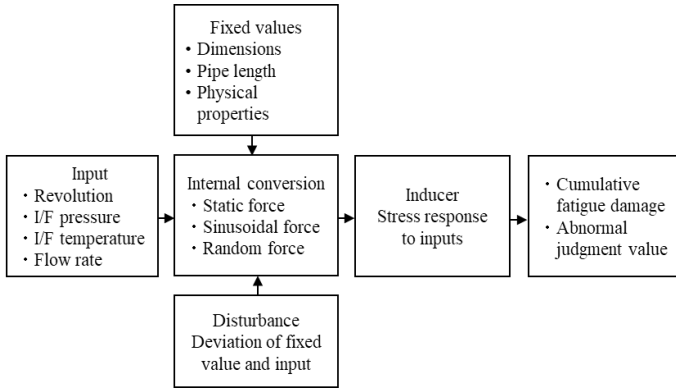


Figure 3. Inducer Remaining Life Prediction system chart

The intensity of pressure emissions caused by cavitation occurrence and disappearance depends on the rotational speed, inlet pressure temperature, and cavitation coefficient. (Figure.4). Therefore, the pressure input into the inducer blade can be considered as a combination of static load, sinusoidal loads, and random loads. Regarding the consumption of life, it is related to the stress response of the inducer blades. The following points outline the content related to this.

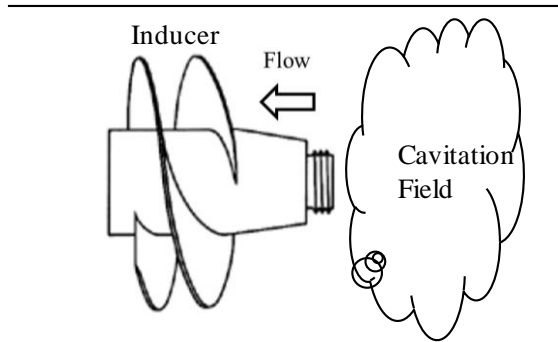


Figure 4. Cavitation generating pressure waves  
Figure borrowed from Brennen (2011)

### 3.3. Stress Response

We consider the stress response of an inducer blade based on the structural eigenvalue sequence  $\omega_i$ . The stress response is defined as the maximum stress value on the blade surface at each eigenvalue  $\omega_i$  to avoid complicating the problem. To derive responses to various inputs, the modal method is applied, allowing each mode to be processed independently. The implementation is done using the Finite Element Method (FEM). In this case, the vibration of the inducer blade is expressed as a superposition of each mode, referring to Nagamatsu (1993)

Individual generalized displacements after mode expansion.

$$\ddot{\xi}_i(t) + 2\zeta_i \omega_i \dot{\xi}_i(t) + \omega_i^2 \xi_i(t) = \Phi_i(t) \quad (3)$$

Here

- $\xi_i$  : Generalized displacements
- $\zeta_i$  : Modal damping ratio
- $\Phi_i(t) = \varphi_i^T f(t)/m_i$  : Generalized force
- $f(t)$ : Force vector
- $\varphi_i$  : i-th mode shape
- $m_i$  : Generalized mass

Fourier transformation of generalized displacement.

$$H_i(\omega) = \frac{\omega_i^2}{\omega_i^2 + 2j\zeta_i \omega_i \omega - \omega^2} \quad (4)$$

Using this model, consider the stress superposition for different mode shapes. We will focus on a single blade in the inducer and combine modes up to a suitable order based on energy distribution. The objective is to find the position where local life consumption is maximized, the point where the combined effect of mean stress and fluctuating stress is highest. We will examine the contribution of frequency bands that generate stress fluctuations and exclude those with small contributions (Figure 5). The average stress, fluctuation value, and magnitude of stress depend on the blade geometry, position, and operating conditions.

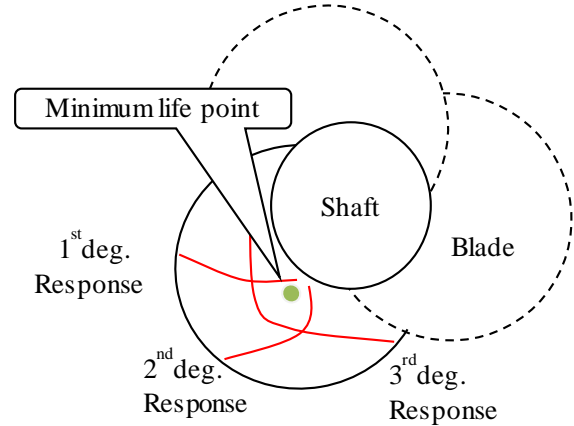


Figure 5. Example of mode shape and life minimum point

The presence of centrifugal forces and pressure differences between the front and back sides of a blade results in the application of average stress (non-zero stress bias) in an inducer. Therefore, it is necessary to perform a life assessment using a modified Goodman diagram.

$$s = s_w \left(1 - \frac{s_m}{s_b}\right) \quad (5)$$

Here

- $s$  : Stress amplitude due to pressure response
- $s_w$  : Fatigue limit for both directions of stress

- $s_m$  : Average stress due to operating conditions  
 (centrifugal forces and pressure differences)  
 $s_b$  : Tensile strength (a material property)

The equivalent stress  $s_s$  applicable for the S-N curve is given by the following equation.

$$s_s = \frac{s}{1 - \frac{s_m}{s_b}} \quad (6)$$

The point where this value becomes the most severe was determined by employing FEM and conducting a survey of the blade surface.

### 3.4. Fatigue Life Consumption

Assuming reference stress amplitude  $s_0$  and reference life  $N_0$ , the predicted life for the applied stress amplitude  $s_s$  can be determined from the S-N curve (Figure 6) as follows.

$$N = N_0 \left( \frac{s_0}{s_s} \right)^b \quad (7)$$

The cumulative fatigue damage when various stress amplitudes  $s_s$  are applied can be calculated using the modified Miner's law as follows:

$$\psi = \sum_i \frac{n_i(s_s)}{N_i(s_s)} \quad (8)$$

Where  $N_i(s_s)$  the initially predicted life is based on the assumed history, and  $n_i(s_s)$  is the consumed life based on the actual history.

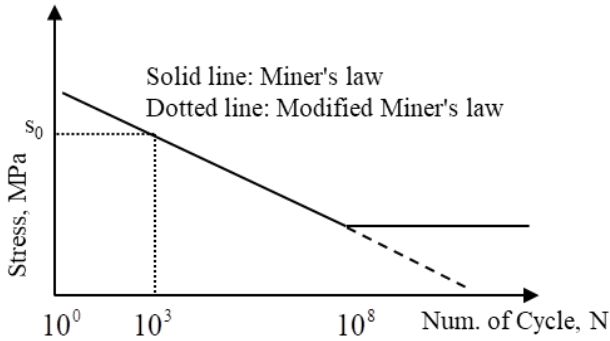


Figure 6. Example image of S-N curve

### 3.5. Estimation of Remaining Life Using the Rain Flow Method

Assuming that the transfer function from pressure fluctuation to stress fluctuation, which corresponds to equation (4), has been obtained through testing, the general response can be expressed as follows, with each transfer function labeled after mode decomposition:

$$H_i(s) = k \frac{\omega_i^2}{\omega_i^2 + 2j\zeta_i\omega_i s + s^2} \quad (9)$$

$k[-]$  : pressure-to-stress conversion factor

Using the measured time-series pressure data  $p_n$  [MPa], the stress response  $\sigma_n$  [MPa] on the airfoil surface for the  $i$ -th eigenvalue at the representative point is expressed by the recursive equation. It is easy to code this equation into a computer.

$$\sigma_{in} = -a_{i1}\sigma_{in-1} - a_{i2}\sigma_{in-2} + b_{i1}p_{n-1} + b_{i2}p_{n-2} \quad (10)$$

The notation for each coefficient is omitted. For example, refer to the following paper, Kanazawa, K., & Matsui, T. (2002).

From this, the actual stress response  $\sigma_n$  can be expressed as follows:

$$\sigma_n = \sum \lambda_i \sigma_{in} + \tilde{\sigma}_n \quad (11)$$

$\lambda_i$  : Contribution of  $i$ -th eigenvalue component

$\tilde{\sigma}_n$  : Steady stress determined by rotation speed, flow rate, cavitation coefficient, etc.

Thus, if the pressure fluctuation  $p_n$  at the upstream reference point and the operating conditions such as rotation speed are known, the stress history  $\sigma_n$  at the airfoil life assessment point can be determined.

Next, assuming that the representative point stress series  $\sigma_n$  has been obtained, the Rain flow method can be applied. The Rain flow method is a technique for extracting information that can be used directly in Miner's law from  $\sigma_n$ . The basic idea is to separate large and small cycles and apply the effect of each to Miner's law in Figure 7. See Okajima, et al (2007) for details. Figures 8 to 11 show this algorithm. At first, it will be selected the sampling interval  $T$  based on the minimum frequency to be evaluated, and the sampling rate  $\Delta T$  based on the maximum frequency to be evaluated.

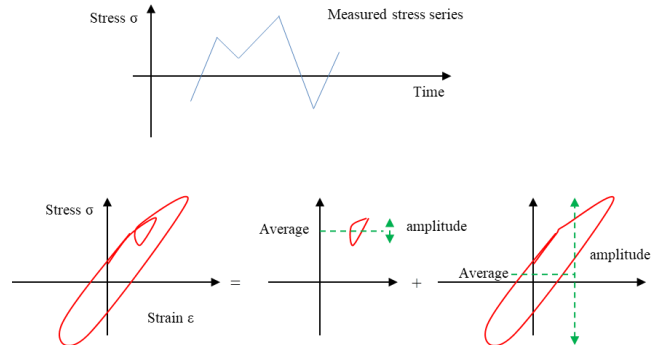


Figure 7. Decomposition of stress series

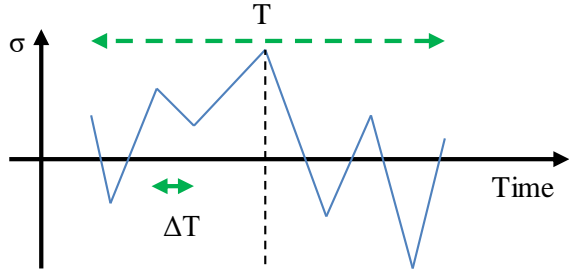


Figure 8. Rain flow Algorithm 1

Next, extract the maximum and minimum values within the interval, divide the maximum value into two halves, and connect the first half to the second half.

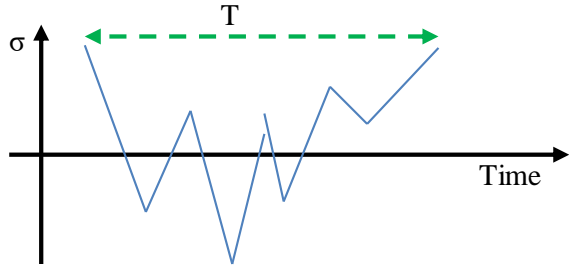


Figure 9. Rain flow Algorithm 2

Then, imagine filling this with water. The amplitude is determined by the difference between the highest and lowest water levels, and the average stress is the middle point.

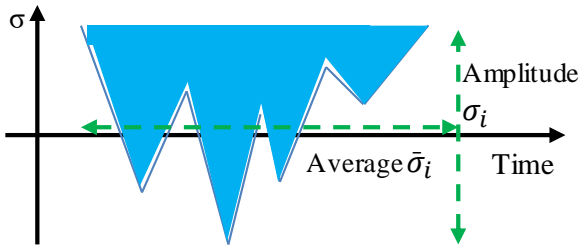


Figure 10. Rain flow Algorithm 3

Then, remove the water from the lowest water level point, and calculate the amplitude and average stress at the new lowest water level point.

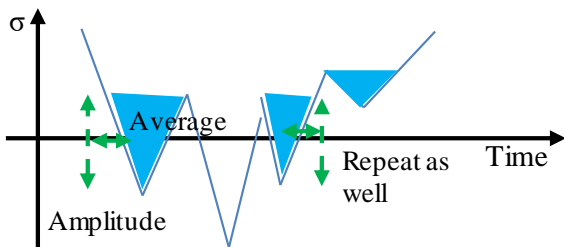


Figure 11. Rain flow Algorithm 4

Repeat this process until the container is empty.

This is known as the Rain flow algorithm, which decomposes the stress sequence into amplitude and mean stress  $(\sigma_i, \bar{\sigma}_i)$ , and calculates the average stress  $S_s$  by substituting it into the modified Goodman diagram equation (6) and the cumulative damage by equation (8) for modified Miner's law.

$$\psi = \sum_i \frac{n_i(s_s(\sigma_i, \bar{\sigma}_i))}{N_i(s_s(\sigma_i, \bar{\sigma}_i))} \quad (12)$$

The rate of change can be obtained by taking the direct difference

$$\dot{\psi} = \frac{\Delta\psi}{\Delta T} \quad (13)$$

$\Delta T$  : Same as the sampling interval

To use it for an actual flight, this process needs to be repeated in real-time.

## 4. EXPERIMENTAL RESULTS AND DISCUSSION

### 4.1. Experiment

From the previous discussion, a mathematical model for predicting residual life has been prepared. However, as shown in Section 3.5, the transfer of stress from the upstream pressure sensor to the inducer blade remained uncertain. Therefore, an attempt was made to obtain the transfer function of that using a test specimen of the inducer. The specimen and the test facility are shown below in Figure 12.

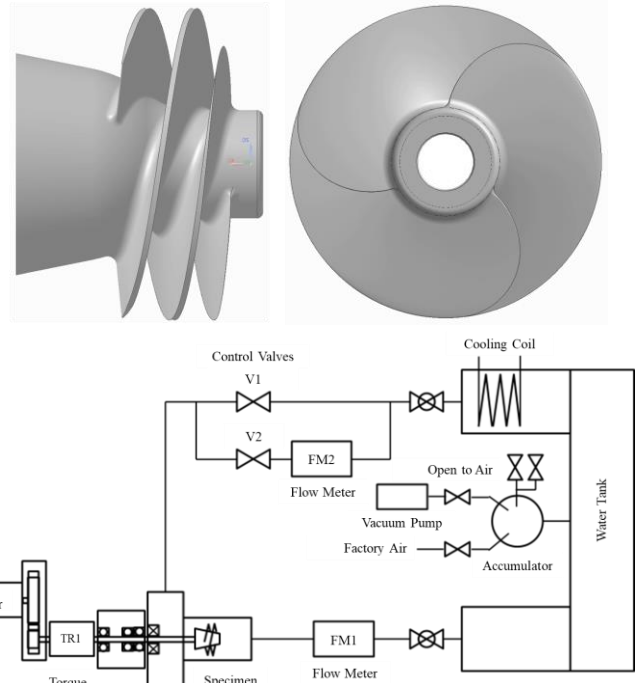


Figure 12. Specimen and Experiment setup



Multiple candidate locations for attaching strain gauges to obtain the response were selected based on the results of the stress analysis and modal analysis mentioned before. Since there are three inducer blades, strain gauges were attached to the same position on each blade. In the strain gauge attachment position diagram (Figure 13), the red circle represents the measurement point that showed the largest strain based on the Rain flow analysis performed using the strain data obtained from the test, which corresponds to the life evaluation point. The sampling frequency was 10 kHz, and the measurement period was 20 seconds. The pressure measurement position was on the side of the piping several tens of millimeters upstream from the leading edge of the inducer blade. Water was used as the working fluid, and the pressure sensor and strain gauge values on the blade surface were recorded while driving the inducer test specimen installed in the circulating fluid loop by a motor under the condition of 7500 rpm.

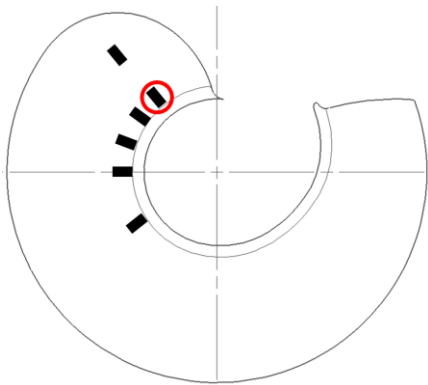


Figure 13. Strain gauge pasting locations

#### 4.2. Result and Discussion

The following Figure 14 is an example of time waveforms for the pressure sensor data and strain gauge data obtained. It appears that almost random waves are predominant.

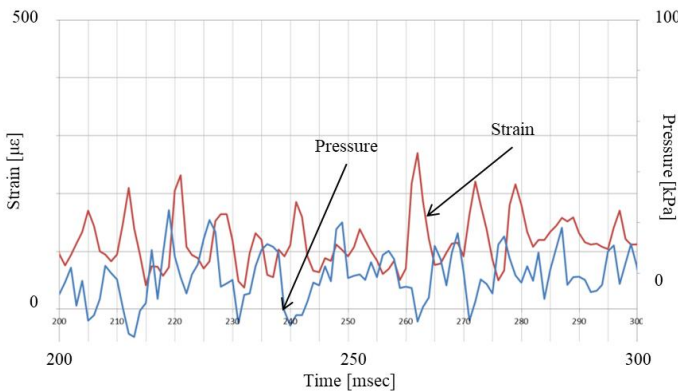


Figure 14. Sample of measured data

The transfer function was calculated from the obtained pressure and strain waveform data. This includes the vibration components consisting of random and sinusoidal waves all at once. An example of gain characteristic from pressure to strain derived from this transfer function is shown in Figure 15.

No particularly large response peaks were observed in the gain characteristic waveforms. The shape of the gain characteristic at the same position on each surface was almost the same, even when the sample interval or the evaluated blade was changed. It was found that similar characteristics could be obtained even for different blades.

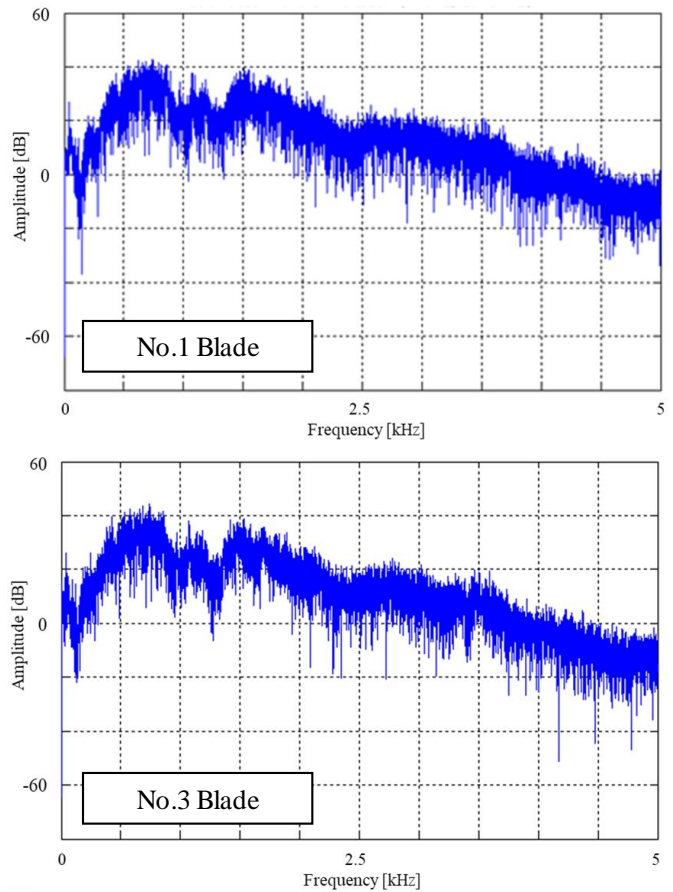


Figure 15. Examples of gain characteristics  
Upper: blade No.1, Lower: blade No.3.

#### 5. CONCLUSION

We attempted to construct a remaining life prediction model for the turbo pump inducer, an important part of rocket engines for future reuse of spacecraft. The goal was to derive stress estimates for the inducer from the pressure sensor signal installed upstream. Through these activities, we achieved certain results in the following areas:

- We constructed a remaining life prediction model by applying modal analysis, Miner's law, and the Rain flow model. At the logic level, we were able to consistently connect from input to output.
- In the process, we verified the correspondence between the most uncertain element, the pressure measurement value, and the stress in the inducer. This was done using water as the working fluid, and a certain degree of practicality was achieved.
  - We can obtain the same transfer function at the same position for the blades of the same shape.
  - We can estimate the blade deformation of the inducer from pressure fluctuations.
- From the above results, it was demonstrated in principle that remaining life prediction is possible based on pressure measurements installed upstream.

However, the following items were recognized as future challenges:

- Acquisition of transfer functions using actual propellants.
- Acquisition of rotational speed sensitivity, temperature sensitivity, and pressure sensitivity.

This activity is planned to continue in the future.

## REFERENCES

- Brennen, C. E. (2011). *Hydrodynamics of pumps*. Cambridge University Press. P37
- Chelouati, M., Jha, M. S., Galeotta, M., & Theilliol, D. (2021, September). Remaining useful life prediction for liquid propulsion rocket engine combustion chamber. In 2021 5th International Conference on Control and Fault-Tolerant Systems (SysTol) (pp. 225-230). IEEE.

- Kanazawa, K., & Matsui, T. (2002). ARMAMA model for spectral analysis and model identification. *Journal of Structural and Construction Engineering, Transactions of AIJ*, 67(554), 71-78.
- Mizuno, T., Kobayashi, S., & Oguchi, H. (2009). Study on a turbo pump for LE-X engine. *IHI Engineering Review*, 49(3), 178-181.
- Nagamatsu, A. (1993). Introduction to mode analysis. 3. Multi-degree-of-freedom systems. Corona Publishing Co., Ltd.
- Okajima, T., Honda, K., Sakai, S., Izumi, S., Ooishi, K., & Kasahara, N. (2007, October). Simplified evaluation guidelines for thermal fatigue damage caused by temperature fluctuations of irregular fluids. In M&M Conference on Materials and Mechanics 2007 (pp. 262-263). The Japan Society of Mechanical Engineers.
- Sato, E. (2019) Elucidation of rapidly-accumulated damage by synergism of ultra-low-cycle fatigue and creep in combustion chamber of rocket engine, 2018 Research Results Report, Grants-in-Aid for Scientific Research

**Hatsuo Mori** received B.S. and M.E. degrees in Applied Mathematics and Physics from Kyoto University and a Ph.D. in Engineering from the University of Tokyo, Japan. His work focuses specifically on the design and development of rocket engines and real-time health monitoring of reusable rocket engines. A regular member of the Design Engineering Division of the Japan Society of Mechanical Engineers. Professional Engineer Japan (Aero-Space).

**Makoto Imamura** received B.S. and M.E. degrees in Applied Mathematics and Physics from Kyoto University and a Ph.D. in Information Science and Technology from Osaka University. After working for Mitsubishi Electric Corp., he became a full professor at Tokai University in April 2016. His research interests include time series analysis, data mining, and PHM. He is a member of IEEE and ACM.